MR Imaging of Lumbar Arachnoiditis

Jeffrey S. Ross, Thomas J. Masaryk, Michael T. Modic, Richard Delamater, Henry Bohlman, Geoffrey Wilbur and Benjamin Kaufman

AJNR Am J Neuroradiol 1987, 8 (5) 885-892
http://www.ajnr.org/content/8/5/885

MR Imaging of Lumbar Arachnoiditis

Jeffrey S. Ross[1]
Thomas J. Masaryk[1]
Michael T. Modic[1]
Richard Delamater[2]
Henry Bohlman[2]
Geoffrey Wilbur[2]
Benjamin Kaufman[1]

To assess the usefulness of MR in defining the changes of lumbar arachnoiditis, we reviewed retrospectively the MR, plain-film myelographic, and CT myelographic findings in 100 patients referred for evaluation of failed-back-surgery syndrome. In 11 of 12 cases of arachnoiditis demonstrated by plain-film and CT myelography, an abnormal configuration of nerve roots was seen by MR. The correlated MR and CT and plain-film myelographic changes were divided into three anatomic groups: group 1 showed conglomerations of adherent roots residing centrally within the thecal sac, group 2 demonstrated roots adherent peripherally to the meninges giving rise to an "empty-sac" appearance, and group 3 demonstrated a soft-tissue mass replacing the subarachnoid space. There was one false-negative MR study.

For the diagnosis of moderate to severe arachnoiditis, we found MR to correlate excellently with CT myelographic and plain-film myelographic findings.

Spinal arachnoiditis is a cause of persistent symptoms in 6–16% of postoperative patients [1]. Its clinical diagnosis is difficult because it has no distinct symptom complex. Previously, the diagnosis of arachnoiditis has been confirmed by myelography and, less commonly, by CT and surgery.

Recently, surface-coil MR imaging with thin slices (less than 5 mm) has been shown to be capable of defining the nerve roots within the thecal sac. We had identified by surface-coil MR what appeared to be arachnoiditis manifested as enlarged or clumped nerve roots in a pattern similar to that seen by CT myelography.

To test the validity of these observations, we undertook a retrospective study of patients referred for evaluation of the failed-back-surgery syndrome who would be at risk for the development of arachnoiditis. Plain-film myelographic and/or CT myelographic studies were used as an objective measure of accuracy. An additional group of patients with no history of spinal instrumentation was also evaluated by surface-coil as a control group.

Materials and Methods

The study group consisted of a retrospective review of 100 patients who had a history of previous lumber spine surgery for disk disease and/or spinal stenosis who were referred for surface-coil MR and plain-film and CT myelographic evaluation of the failed-back-surgery syndrome. Of the 12 patients with CT and plain-film myelographic findings of arachnoiditis, MR studies were performed within 24 hr in eight cases, within 1–6 months in two cases, and within 2 years in two cases. In these last four cases, no changes in symptomatology occurred in the interval between CT/plain-film myelography and surface-coil MR studies.

The MR examinations were performed on 1.0- or 1.5-T superconductive units (Siemens Magnetom) with a copper foil–wrapped circular surface coil operating in the receive mode. A 50-cm body coil served as the radiofrequency transmitter. A complete study consisted of five acquisitions. Patient positioning and coil placement were first determined with a coronal study by using a repetition time (TR) of 500 msec and an echo time (TE) of 30 msec, 1-cm slice

This article appears in the September/October 1987 issue of *AJNR* and the November 1987 issue of *AJR*.

Received January 15, 1987; accepted after revision April 1, 1987.

[1] Department of Radiology, University Hospitals of Cleveland, Case Western Reserve University, Cleveland, OH 44106. Address reprint requests to J. S. Ross.

[2] Department of Orthopedic Surgery, University Hospitals of Cleveland, Case Western Reserve University, Cleveland, OH 44106.

***AJNR* 8:885–892, September/October 1987**
0195–6108/87/0805–0892

thickness, 128 × 128 acquisition matrix, and one excitation. Total examination time was 1.1 min. Two axial- and two sagittal-plane acquisitions were obtained with a slice thickness of 4 mm, 2-mm interslice gap, and 256 × 256 or 256 × 512 acquisition matrix, yielding a 0.9- by 0.9-mm or 0.9- by 0.45-mm pixel size, respectively. The sagittal sequences were TR = 500–700 msec/TE = 17–30 msec (T1-weighted) with two excitations, and TR = 2000 msec/TE = 90 msec (T2-weighted) with one excitation. Axial T1-weighted images were obtained with TR = 500–1000 msec/TE = 17–30 msec and two excitations. Intermediate (TR = 2000 msec/TE = 30 msec) and T2-weighted (TR = 2000 msec/TE = 90 msec) images were acquired with an asymmetric multiecho sequence with one excitation. All data were collected in the two-dimensional Fourier transform mode. Total examination time was 35–45 min.

The comparative myelographic studies were performed with a 22-gauge spinal needle with instillation of 10–12 ml of metrizamide (190 mg I/ml) intrathecally or 10–15 ml of iohexol (180 mg I/ml). Routine anteroposterior, lateral, and oblique views were obtained. Subsequent CT examinations were performed 4 hr after the myelogram with a Siemens DRH scanner operating at 125 kVp with a 4-mm slice thickness. The surface-coil MR study and plain-film myelogram and/or CT myelogram studies were evaluated independently by two of us, without knowledge of the results of the other studies.

The surface-coil MR studies were evaluated for (1) the appearance of the dural tube on axial and sagittal images, (2) the appearance and location of the intrathecal lumbar nerve roots, and (3) signal-intensity changes of the thecal sac or nerve roots. The CT myelograms were evaluated in a manner similar to (1) and (2) above, with the exception that only axial images were obtained. The plain-film myelograms were evaluated for features of arachnoiditis including (1) blunting of the nerve-root sleeves, (2) lack of visibility or clumping of nerve roots, (3) irregularity of the thecal sac, and (4) myelographic block.

The control-group patients were identified as patients referred for an MR study for back pain with no previous history of myelography or spinal surgery. Ten of these 20 patients had a plain-film and/or CT myelogram within 1 week of the surface-coil MR study. These MR studies were also interpreted independently of the plain-film/CT myelography studies.

Results

Controls

None of the 20 patients in the control group had changes suggestive of arachnoiditis. A sampling of the variable appearances of the normal lumbar roots by surface-coil MR is presented in Figure 1. A total of 54 axial vertebral body levels were examined in this group with a distribution as follows: L2, three; L3, 12; L4, 20; and L5, 19. At the L2 level, the roots were seen as a mass of soft-tissue signal in the dependent portion of the thecal sac. The roots assumed a smooth crescentic appearance after the curvature of the thecal sac. The common pattern of the nerve roots at the L3 level was one of a group of roots amassed posteriorly (dependent position), which was crescentic and smooth, or more globular and irregular in appearance. The roots about to exit the dural tube were placed anterolaterally in a symmetric pattern. At the L4 level, the roots were often dispersed enough that they were seen as separate delicate entities, arranged in a symmetric pattern within the CSF. By the L5 level, the few roots present were equally spaced from one another within the thecal sac. A pattern of conglomeration within the center of the thecal sac was conspicuously lacking at this level. While the nerve roots were visible on T1-weighted images, they were appreciated most easily against the background of high signal provided by T2-weighted images.

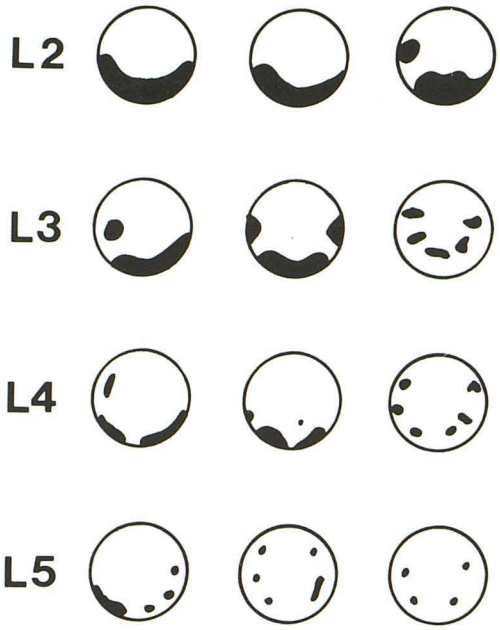

Fig. 1.—Variable appearance of normal lumbar nerve roots on axial T1-weighted images, by vertebral body level.

Midline sagittal images showed the roots as a single band of intermediate signal intensity following the posterior thecal sac. The band of roots gradually tapered from the conus to the L4 level. Parasagittal images showed the roots dispersing in a fan-shaped manner as they traveled anteroinferiorly.

Postoperative Patients

Of the 100 patients examined, 12 had CT and plain-film myelographic changes of arachnoiditis. In 11 of these cases, surface-coil MR demonstrated a pattern of nerve roots that was believed to be abnormal (based on the criteria established by the control group) and consistent with arachnoiditis. The correlated surface-coil MR/CT myelography/plain-film myelography morphologic changes were divided into three groups.

Group 1.—In this group (three patients), the predominant surface-coil MR findings were large conglomerations of nerve roots residing centrally within the thecal sac (Fig. 2). No peripheral dural thickening was seen. The nerve roots were seen on T1-weighted images as rounded areas of soft-tissue signal. Improved definition of the clumped nerve roots was seen with the high contrast provided by the high CSF signal on T2-weighted images. The CT myelographic appearance was similar to that of the T2-weighted surface-coil MR images, showing central thickening of the nerve roots. Again, no focal or diffuse dural thickening was seen. The myelograms varied in appearance from loss of definition of the root sleeves with

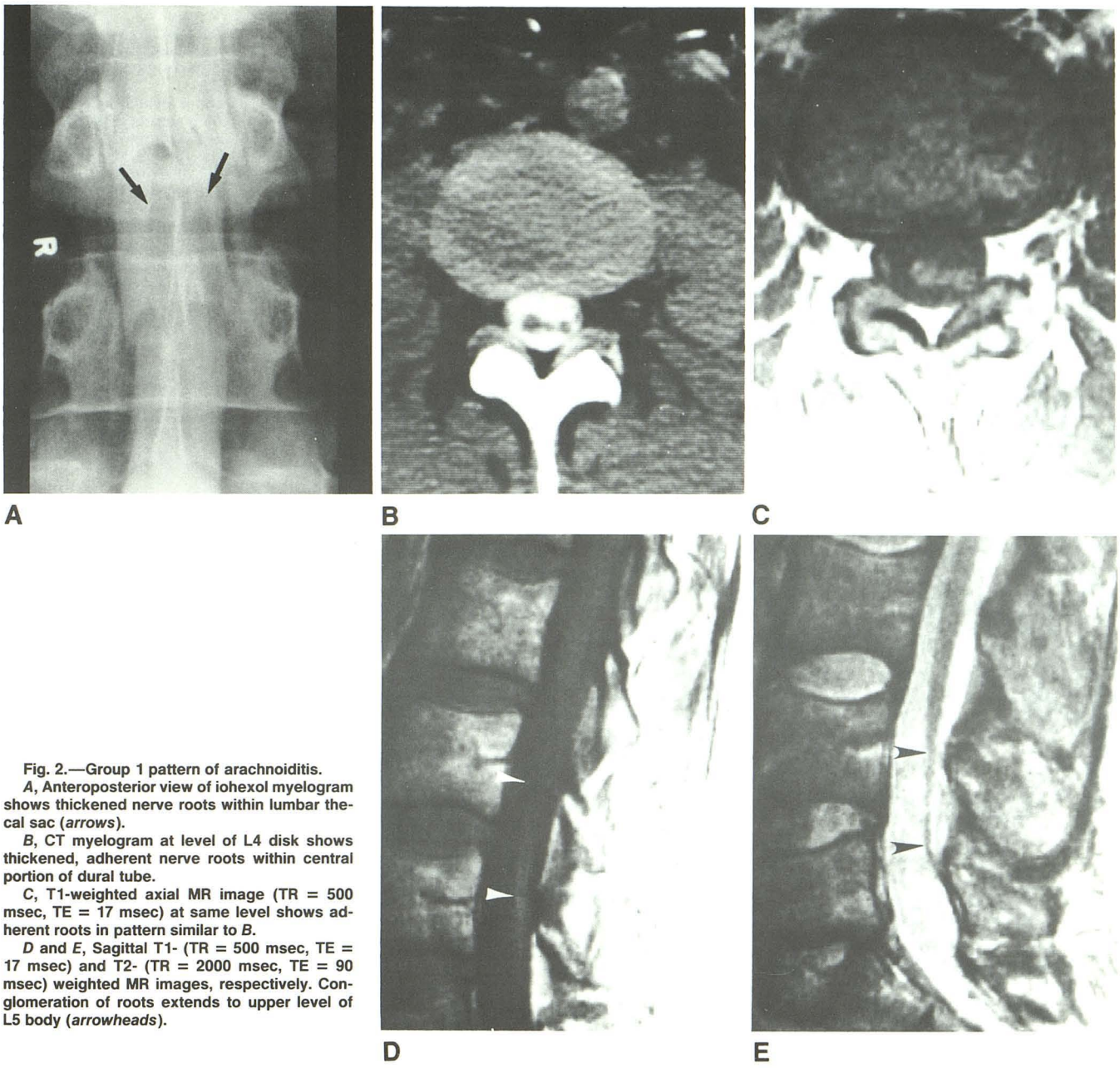

Fig. 2.—Group 1 pattern of arachnoiditis.

***A*, Anteroposterior view of iohexol myelogram shows thickened nerve roots within lumbar thecal sac (*arrows*).**

***B*, CT myelogram at level of L4 disk shows thickened, adherent nerve roots within central portion of dural tube.**

***C*, T1-weighted axial MR image (TR = 500 msec, TE = 17 msec) at same level shows adherent roots in pattern similar to *B*.**

***D* and *E*, Sagittal T1- (TR = 500 msec, TE = 17 msec) and T2- (TR = 2000 msec, TE = 90 msec) weighted MR images, respectively. Conglomeration of roots extends to upper level of L5 body (*arrowheads*).**

thickened roots seen intrathecally to moderate narrowing and irregularity of the contrast column.

Group 2.—In this group (five patients), surface-coil MR demonstrated clumped nerve roots attached peripherally to the meninges (Fig. 3). This appeared as focal thickening of the meninges, with few or no nerve roots visible within the subarachnoid space. T2-weighted images provided the best definition of the peripheral nerve roots and the central homogeneous CSF. The appearance was essentially one of an "empty thecal sac." The CT myelograms also showed focal thickening of soft-tissue attenuation peripherally along the meninges. The central portion of the subarachnoid space showed homogeneous contrast with few or no nerve roots. The myelograms showed a capacious thecal sac with a smooth outer border, amputation of the root sleeves, and no nerve roots visible within the caudal thecal sac.

One additional patient demonstrated findings of both groups 1 and 2, with central clumping of the roots at the L4 level progressing to peripheral adhesions of the roots to the meninges at the L5 level.

Group 3.—In this group (two patients), T1-weighted surface-coil MR images demonstrated increased soft-tissue signal within the thecal sac below the conus medullaris, obliterating centrally the majority of the subarachnoid space (Fig.

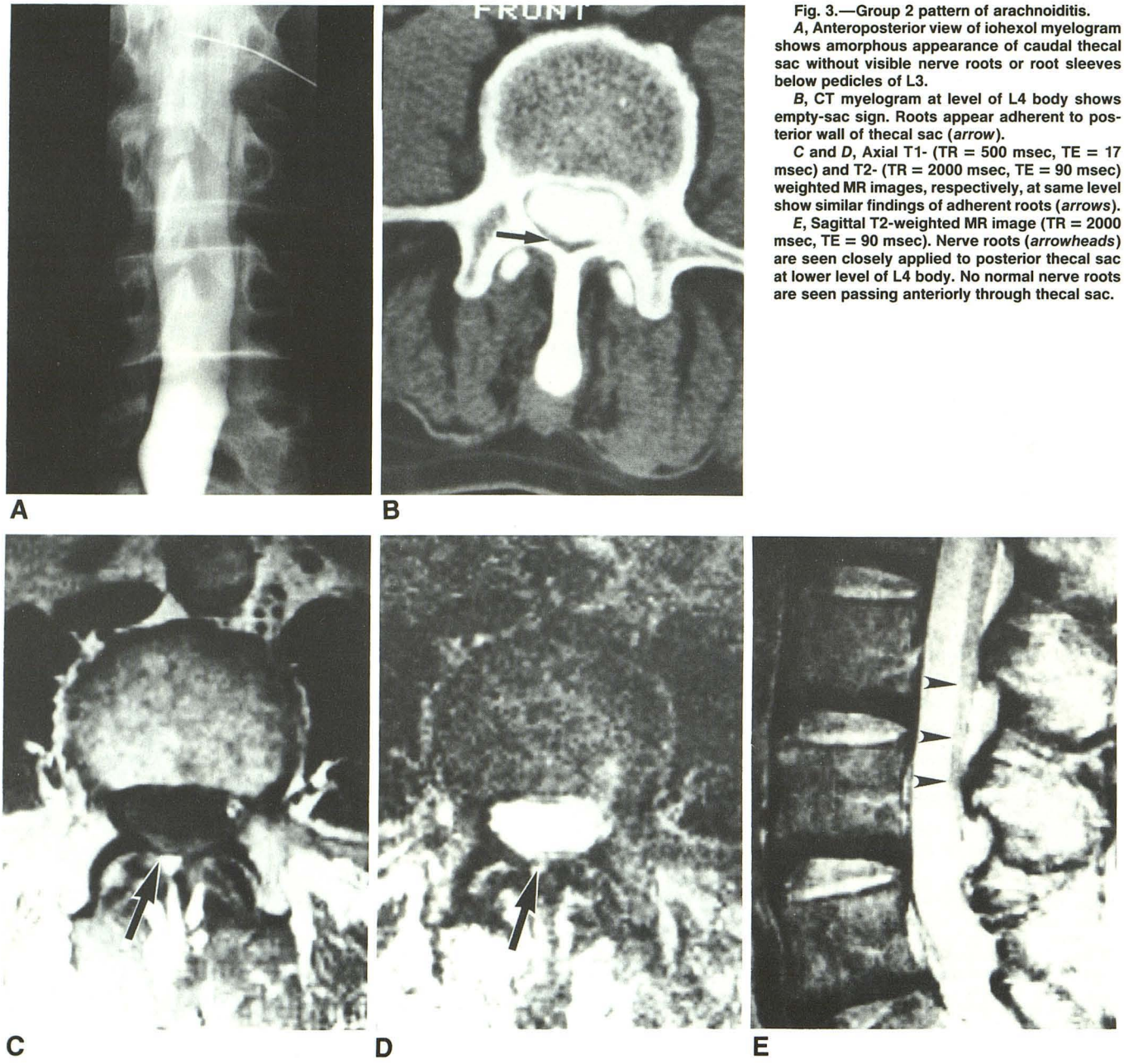

Fig. 3.—Group 2 pattern of arachnoiditis.
***A*, Anteroposterior view of iohexol myelogram shows amorphous appearance of caudal thecal sac without visible nerve roots or root sleeves below pedicles of L3.**
***B*, CT myelogram at level of L4 body shows empty-sac sign. Roots appear adherent to posterior wall of thecal sac (*arrow*).**
***C* and *D*, Axial T1- (TR = 500 msec, TE = 17 msec) and T2- (TR = 2000 msec, TE = 90 msec) weighted MR images, respectively, at same level show similar findings of adherent roots (*arrows*).**
***E*, Sagittal T2-weighted MR image (TR = 2000 msec, TE = 90 msec). Nerve roots (*arrowheads*) are seen closely applied to posterior thecal sac at lower level of L4 body. No normal nerve roots are seen passing anteriorly through thecal sac.**

4). T2-weighted images showed increased signal diffusely from the thecal sac without definition of individual nerve roots. CT myelography showed increased soft-tissue attenuation material within the subarachnoid space with small loculated areas of contrast material peripherally. Myelography demonstrated blocks of the subarachnoid space in both patients, with the distal visualized subarachnoid space being irregular and assuming a "candle-dripping" appearance.

There was one false-negative surface-coil MR study. In this patient, arachnoiditis seen on plain-film and CT myelography (in a group 2 pattern) was not seen on surface-coil MR (Fig. 5). Instead, MR showed inhomogeneous signal from the thecal sac, but no definite empty sac or central clumping.

In all the cases, the abnormalities were seen at the L3 level or below. In all 11 patients the abnormal configurations of the nerve roots in the lumbar spine were seen over at least two vertebral-body levels (Table 1).

Discussion

The pathogenesis of spinal arachnoiditis is similar to the repair process of serous membranes, such as the peritoneum,

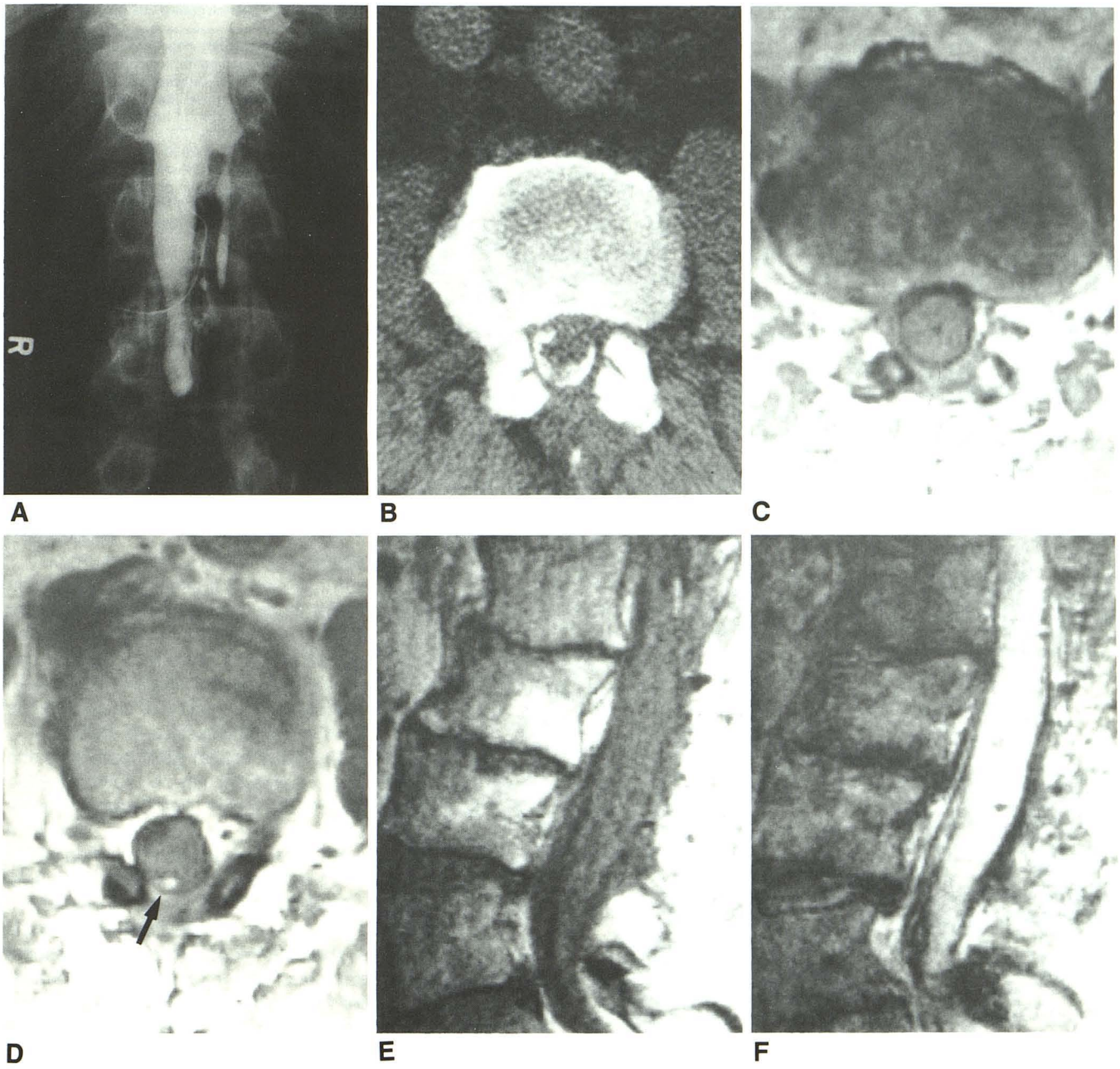

Fig. 4.—Group 3 pattern of arachnoiditis.

***A*, Anteroposterior view of iohexol myelogram via C1–C2 puncture. There is block at inferior level of L2 body, with candle-dripping appearance of distal contrast material. Note previous laminectomy and small epidural wire from dorsal column stimulation for pain control.**

***B*, CT myelogram at L3 level. Soft-tissue attenuation mass fills much of lumbar thecal sac. *C*, Axial T1-weighted MR image (TR = 500 msec, TE = 17 msec) at same level. Thecal sac is nearly filled with mass of intermediate signal. CSF signal is present as peripheral rim about mass and in small central collection.**

***D*, Axial T1-weighted MR image (TR = 500 msec, TE = 17 msec) at L2 level. Adherent roots are also visible at this level, as well as small area of high signal from residual Pantopaque (*arrow*).**

***E*, Sagittal T1-weighted MR image (TR = 500 msec, TE = 17 msec). Abnormal mass of intermediate signal is present throughout lumbar thecal sac.**

***F*, Sagittal T2-weighted MR image (TR = 2000 msec, TE = 90 msec). High signal within dural tube does not allow distinction between normal CSF and arachnoiditis.**

with a negligible inflammatory cellular exudate and prominent fibrinous exudate. The fibrin-covered roots stick to themselves as well as to the thecal sac. Eventually, dense collagenous adhesions are formed by proliferating fibrocytes during the repair phase [2].

Myelography in chronic spinal arachnoiditis produces a variety of patterns including prominent cauda equina nerve roots, a homogeneous contrast pattern without root shadows, and subarachnoid filling defects with narrowing and shortening of the thecal sac. Jorgensen and Hansen [3]

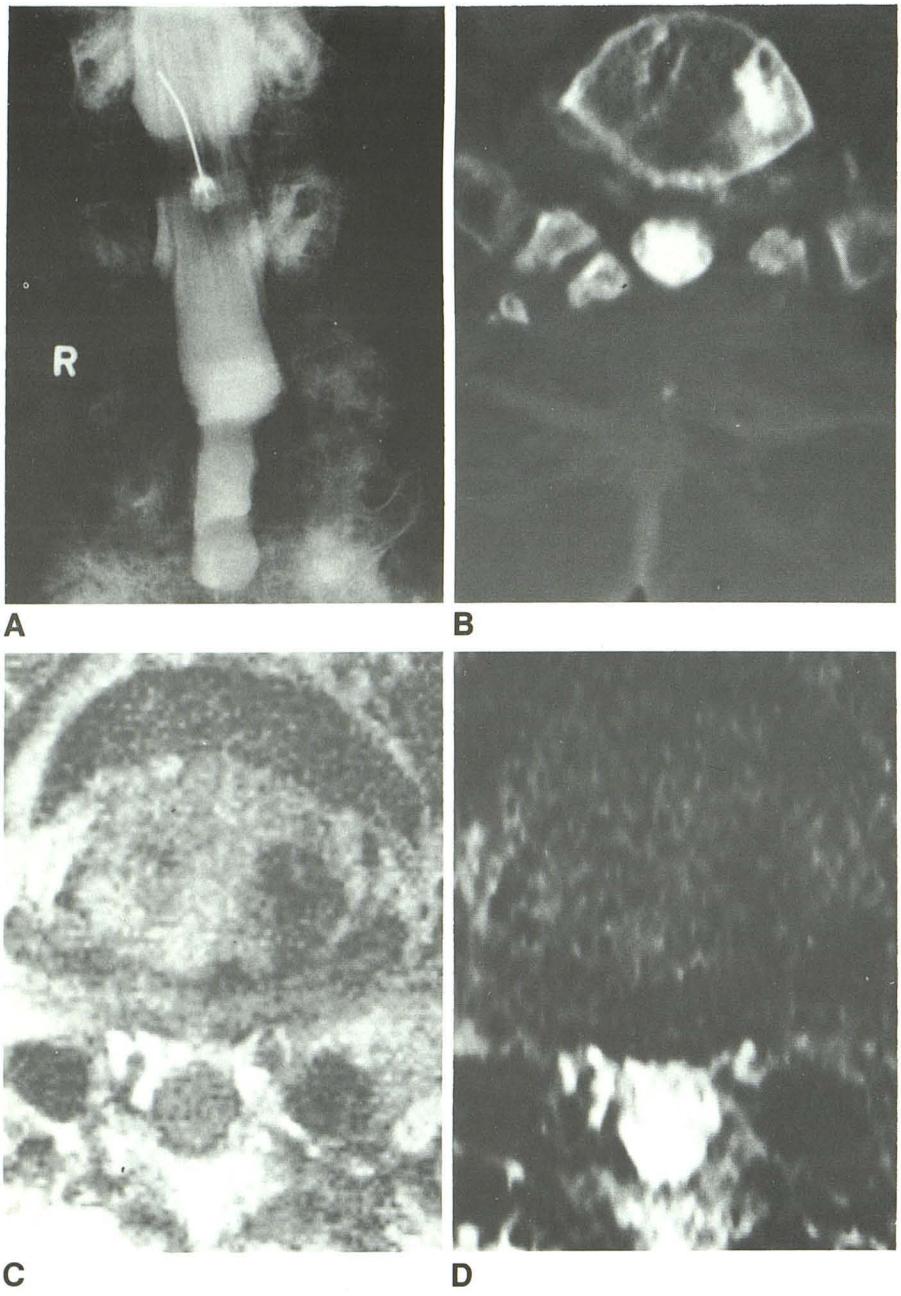

Fig. 5.—False-negative MR finding of arachnoiditis.

***A*, Anteroposterior view of iohexol myelogram shows amorphous collection of contrast material in distal thecal sac representing arachnoiditis.**

***B*, CT myelogram at L5 level shows abnormal peripheral distribution of nerve roots.**

***C* and *D*, Axial T1- (TR = 500 msec, TE = 17 msec) and T2- (TR = 2000 msec, TE = 90 msec) weighted MR images. Poor signal to noise does not allow demonstration of abnormal nerve-root morphology. Low signal lateral to dural tube is acrylic cement from previous posterior spinal fusion.**

divided the myelographic patterns into two groups: type 1 is caused by an adhesion of the roots inside the meninges, giving a root "sleeveless" appearance. Type 2 demonstrated filling defects, narrowing, shortening, and occlusion of the thecal sac. Type 1 appears to be mild disease; type 2 is the picture of more extensive adhesions [3, 4]. With CT myelography, early adhesions are seen in the distal thecal sac as a loss of root-sleeve filling. Roots will become adherent to one another and to the dura, leading to the appearance of an empty sac [5]. As the transmeningeal fibrosis continues, the clumping becomes more prominent until the thecal sac and roots are one soft-tissue mass. This produces a myelographic block, and has been considered the "end stage" of arachnoiditis [6].

In this series we identified the surface-coil MR appearances of arachnoiditis in 11 of 12 cases demonstrated by CT myelography and plain-film myelography. This represents a sensitivity of 92%, specificity of 100%, and accuracy of 99%. The surface-coil MR appearance of arachnoiditis was equivalent to the changes demonstrated by CT myelography. Central and peripheral adhesions of roots were the most common patterns. Central clumping (group 1) demonstrated large conglomerations of roots residing centrally in the dural tube. Peripheral adhesions (group 2) gave rise to an empty-sac

TABLE 1: Levels Involved by Arachnoiditis on MR

Type: Case No.	Levels
1, Conglomerations of adherent roots centrally within thecal sac:	
1	L3–S1
2	L3–S1
3	L4–S1
4[a]	L4
2, Roots adherent peripherally to meninges:	
4[a]	L5
5	L3–S1
6	L3–S1
7	L3–S1
8	L4–L5
9	L5–S1
3, Soft-tissue mass replacing subarachnoid space:	
10	L4–S1
11	L2–S1

[a] The findings of two groups were present in this patient.

appearance, which was especially evident on T2-weighted axial images.

Our groups 1 and 2 patients fall within the type 1 category defined by Jorgensen and Hansen [3], the difference being the distinction between central and peripheral clumping of the nerve roots. The more severe disease, (Jorgenson and Hansen type 2) is reflected in our group 3, showing soft tissue replacing the subarachnoid space on CT and surface-coil MR and giving rise to a block on myelography.

The failure of surface-coil MR to diagnose arachnoiditis in one case most likely relates to poor image quality caused by patient motion. At our institution, T2-weighted images are usually acquired last, when patient fatigue and motion are maximum.

The normal appearance of the nerve roots at the L2 or L3 level could potentially be mistaken for arachnoiditis. In practice, however, this was not a problem, since in our groups arachnoiditis involved the L3 level and below, and also extended over at least two lumbar-body levels. The diagnosis of arachnoiditis should not be made on one axial image, but necessitates the visual integration of the appearance of the roots over several levels. Clumping of lumbar nerve roots will be seen with spinal stenosis, which could mimic a group 3 type of arachnoiditis. However, associated bony and ligamentous findings allow a correct diagnosis. The distinction between tumor and group 3 arachnoiditis may be impossible by MR, except for the secondary findings of previous surgery and/or Pantopaque myelography. Neoplastic CSF seeding could produce adhesions of the nerve roots indistinguishable from group 1 changes. However, the roots seen in group 1 arachnoiditis were generally smooth and tapered, in contrast to the focal, irregular tumor collections seen with CSF seeding.

The most efficient sequence for imaging arachnoiditis is probably the axial T1-weighted sequence. It allows confidence in defining all three groups of arachnoiditis. A recent report has addressed the inability of heavily T2-weighted sequences to distinguish inflammatory tissue (such as arachnoiditis) within the thecal sac with body-coil MR [7]. In our experience with surface-coil MR, the T2-weighted axial study was helpful in defining the distribution of roots in the thecal sac with greater contrast than was provided by T1-weighted images, at least for groups 1 and 2. However, the pathology of group 3 may potentially be masked on the T2-weighted study because of high signal from the fibrosis and adhesions mimicking normal CSF signal.

The causes of spinal arachnoiditis are varied and include infection, intrathecal steroids or anesthetic agents, trauma, surgery, and intrathecal hemorrhage [8]. All our patients had previous surgery. Retained Pantopaque was present in three patients (one each in groups 1, 2, and 3) and showed increased signal on T1-weighted images and low signal on T2-weighted images [9, 10]. One patient in group 1 received intrathecal steroids. It is not the purpose of this article to correlate postoperative symptomatology with the presence or absence of arachnoiditis, surgical type, or time interval since surgery. Rather, we have identified the morphologic changes of arachnoiditis by MR and correlated them with CT and plain-film myelography.

Our groupings of the appearance of arachnoiditis by MR are by anatomic appearance and are not meant to imply discrete pathologic stages. Arachnoiditis is a dynamic process involving a spectrum of collagen deposition and fibrosis, ranging from minimal changes such as contrast enhancement of the dural tube or clumping of two or three roots to a soft-tissue mass involving roots and meninges [11]. In this study, we found no subtle cases of arachnoiditis by MR or CT or plain-film myelography. Whether MR can detect minimal nerve-root changes of arachnoiditis remains to be determined. Thickening of the posterior meninges, while potentially present, could not be seen because of the contiguous posterior epidural scarring that masks the outer margin of the dural tube. Nevertheless, for the diagnosis of moderate to severe arachnoiditis, surface-coil MR correlates excellently with CT myelographic and plain-film myelographic findings.

ACKNOWLEDGMENT

We thank Helen Kurz for secretarial assistance in manuscript preparation.

REFERENCES

1. Burton CV, Kirkaldy-Willis WH, Yong-Hing K, Heithoff KB. Causes of failure of surgery on the lumbar spine. *Clin Orthop* **1981**;157:191–199
2. Smolik E, Nash F. Lumbar spinal arachnoiditis: a complication of the intervertebral disc operation. *Ann Surg* **1951**;133:490–495
3. Jorgensen J, Hansen PH, Steenskov V, Ovesen N. A clinical and radiological study of chronic lower spinal arachnoiditis. *Neuroradiology* **1975**;9:139–144
4. Smith RW, Loeser JD. A myelographic variant in lumbar arachnoiditis. *J Neurosurg* **1972**;36(4):441–446
5. Simmons JD, Newton TH. Arachnoiditis. In: Newton TH, Potts DG, eds. *Computed tomography of the spine and spinal cord*. San Anselmo, CA: Clavadel, **1983**:223–229
6. Quencer RM, Tenner M, Rothman L. The postoperative myelogram. *Radiology* **1977**;123:667–679

7. Reicher MA, Gold RH, Halbach VV, Rauschning W, Wilson GH, Lufkin RB. MR imaging of the lumbar spine: anatomic correlations and the effects of technical variations. *AJR* **1986**;147:891–898
8. Quiles M, Marchisello PJ, Tsairis P. Lumbar adhesive arachnoiditis, etiologic and pathologic aspects. *Spine* **1978**;3(1):45–50
9. Braun IF, Malko JA, Davis PC, Hoffman JC Jr, Jacobs LH. The behavior of Pantopaque on MR: in vivo and in vitro analyses. *AJNR* **1986**;7:997–1001
10. Marnourian AC, Briggs RW. Appearance of Pantopaque on MR images. *Radiology* **1986**;158:457–460
11. Teplick JG, Haskin ME. Computed tomography of the postoperative lumbar spine. *AJNR* **1983**;4:1053–1072, *AJR* **1983**;141:865–884